SAFE SPACECRAFT SWARM DEPLOYMENT AND ACQUISITION IN PERTURBED NEAR-CIRCULAR ORBITS SUBJECT TO OPERATIONAL CONSTRAINTS

Adam W. Koenig* **and Simone D'Amico†**

This paper presents a set of deployment and formation acquisition procedures for spacecraft swarms in perturbed near-circular orbits subject to operational constraints. Specifically, two open-loop command sequences are developed that allow a mothership to deploy a large number of deputies into passively safe formations. These formations guarantee a user-specified minimum separation between all spacecraft in either the orbit plane or the plane perpendicular to the flight direction. Following the open-loop deployment sequence, all deputies are required to passively drift for a specified time in order to accommodate commissioning operations such as de-spin and sensor and actuator calibration. At the end of the commissioning phase, a nonlinear low-thrust control law is engaged to acquire the desired formation and counteract any errors introduced in the deployment sequence. Additionally, analytical lower bounds on the duration of the passively safe relative motion after deployment are derived as functions of control error parameters. These bounds can be used to define error requirements for the deployment system and specify the duration of the commissioning phase to ensure passive collision avoidance until actuation capabilities are established. The proposed deployment and formation acquisition procedures are validated through simulations using a high-fidelity numerical orbit propagator. The results of these simulations demonstrate that the proposed procedures provide a robust means of establishing safe swarm formations at low delta-v cost in low earth orbit.

INTRODUCTION

Following the successes of missions such as GRACE (NASA),[1] TanDEM-X (DLR),[2] and MMS (NASA),[3] spacecraft formation flying has proven to be a critical technology in earth and space science. Use of multiple spacecraft enables capabilities that are difficult or impossible to achieve using a single monolithic spacecraft and adds a degree of fault tolerance to mission designs. While a malfunction on a monolithic spacecraft commonly results in mission failure, spacecraft formations may be able to tolerate loss of one spacecraft by distributing the workload among the remaining vehicles. Due to this robustness, there is now a growing interest in spacecraft swarms, or formations consisting of a large number of small, low-cost spacecraft. These swarms may enable missions that require massively distributed sensing capabilities such as distributed antennas or sparse aperture arrays. In order to provide a competitive advantage over a binary formation or monolithic spacecraft, the spacecraft employed in a swarm mission must be smaller and cheaper. In particular, the commonly considered platforms for swarm missions are nano- or femto-satellites.[4] These spacecraft have limited onboard sensing, actuation, and computation resources. Additionally, the collision avoidance problem is much more challenging for spacecraft swarms than binary formations due to the large number of vehicles.

At present, only a small body of literature exists on guidance, navigation, and control (GN&C) of multi-agent systems that addresses the computation and actuation limitations that characterize spacecraft swarm missions. The majority of these works focus on three topics: 1) identification of scalable formations that

*Ph.D. Candidate, Department of Aeronautics and Astronautics, Stanford University, 496 Lomita Mall, Stanford, CA, 94305
†Assistant Professor, Department of Aeronautics and Astronautics, Stanford University, 496 Lomita Mall, Stanford, CA, 94305

exhibit passively bounded relative motion and collision avoidance,[5–7] 2) formation-keeping control laws,[6,7] and 3) formation reconfiguration.[8–11] To enable the proposed swarm missions, it is also necessary to study the initial mission phases from separation from the launch vehicle to the start of nominal operations. There are numerous studies that address these mission phases for binary formations such as GRACE[12] and PRISMA.[13] The most relevant demonstration to date with respect to the limitations of spacecraft swarms was the ejection of a pico-satellite target from the BIROS (DLR) spacecraft for the AVANTI experiment.[14] The objective of this study was to identify an open-loop deployment procedure ensures that the pico-satellite does not drift out of range of the sensor for the experiment without compromising the safety of the BIROS spacecraft. However, deployment of a spacecraft swarm is a more challenging problem because of the large number of vehicles. The deployment and formation acquisition procedure for a spacecraft swarm mission must satisfy five key requirements. First, the spacecraft must not collide. Second, the passive relative motion of the swarm must be bounded to accommodate the limited communication capabilities of small spacecraft. Also, the constraints imposed by the bounded relative motion and collision avoidance requirements are effectively contradictory because the simplest method to ensure collision avoidance is to ensure that the spacecraft have different orbit energies, causing them to drift apart. Third, the procedure must be robust to realistic control errors. Fourth, operational constraints of the deployed spacecraft must be accommodated. While operational constraints vary widely between missions, a common constraint is that deployed spacecraft require a commissioning phase to allow for operations such as de-spin and sensor and actuator calibration. During this time the spacecraft cannot be actively controlled. Thus, the relative motion after deployment must be passively safe for sufficient time to allow the deputies to perform commissioning operations. Fifth, the procedure should be scalable to allow deployment of a large number of spacecraft. To date, the deployment and formation acquisition problem for spacecraft swarms is largely unexplored in literature and the few available studies only address a subset of these requirements. Specifically, Boutonnet describes a series of delta-v optimal maneuvers that can establish a small swarm in a stable relative orbit about a reference object, but operational constraints and maneuver execution errors are not addressed.[15] Instead, Jiang presents a means of obtaining stable relative orbits using only a spring-based deployment mechanism, but errors are assumed to be very small and collision avoidance is neglected. Also, neither of these studies provides any evidence that the method can be scaled to accommodate a larger number of spacecraft. Indeed, to date no study has produced a solution to the problem of deployment and formation acquisition for spacecraft swarms that meets all five of the key requirements.

To meet this need, this paper presents for the first time in literature a set of deployment and formation acquisition procedures for spacecraft swarms that meets all five of the aforementioned requirements. To accomplish this goal, this paper builds on the foundation laid by a recent study on guidance and control of spacecraft swarms,[7] which produced two key findings. First, two classes of swarm formations based on relative orbital elements (ROE) were developed that provide safe and bounded relative motion in perturbed near-circular orbits. The first formation class, hereafter called an in-plane formation, provides a user-specified minimum separation between all spacecraft in the orbit plane. In-plane formations maximize the number of spacecraft that can be deployed in a specified volume. However, the cost of this property is that the collision avoidance constraints are functions of the mean separation in the flight direction. As such, these formations require frequent control to counteract the effects of differential drag and maneuver execution errors. Instead, the second formation class, hereafter called an eccentricity/inclination (e/i) vector separation formation, guarantees a user-specified minimum separation in the plane perpendicular to the flight direction. These formations use a generalized form of D'Amico's e/i vector separation concept[16] that accommodates an arbitrary number of spacecraft. The main advantage of this formation is that the collision avoidance constraints are not functions of the mean separation in the flight direction. As a result, passively safe relative motion can be guaranteed for several days in orbits perturbed by both J_2 and differential drag. Second, it was found that in-plane ROE must be periodically controlled for both of these formations to counteract the effects of differential drag. To accomplish this, a set of simple nonlinear state space control laws was developed that use actuation in only the (anti-)flight direction. This paper complements these findings by providing a safe and robust means of deploying a spacecraft swarm into each of these formations subject to realistic control errors and operational constraints. Specifically, this paper makes three contributions to the state-of-the-art. First, two open-loop command sequences are presented that allow a mothership to deploy a large number of deputies into an in-plane or e/i vector separation formation. These procedures simultaneously ensure collision avoid-

ance and minimize the passive drift between all spacecraft in the swarm. Second, analytical lower bounds on the duration of the passively safe relative motion after deployment are derived as functions of control error parameters. These bounds are used to specify error requirements for the deployment system and determine the allowable duration of the commissioning phase for each deputy. Third, the deployment and formation acquisition procedures are validated through simulations using a high-fidelity orbit propagator including all relevant perturbations in low earth orbit (LEO) as well as realistic navigation and control errors. The results of these simulations demonstrate that the proposed procedures can safely establish swarm formations in LEO at low delta-v cost including realistic errors and operational constraints.

After this introduction, key findings on formation design, guidance, and control of spacecraft swarms from a recent work by the authors are reviewed.[7] Next, the deployment procedures for each of the two swarm formation classes are presented and analytical lower bounds on the duration of passively safe relative motion after ejection are derived. Finally, a set of simulations is performed using a high-fidelity numerical orbit propagator to validate the performance of the proposed procedures.

BACKGROUND: SWARM FORMATION DESIGN, GUIDANCE, AND CONTROL

In this paper, a spacecraft swarm is modeled as a mothership with N deputies that uses the operations concept outlined in the following. After separation from the launch vehicle, the mothership performs its required commissioning operations. Next, the mothership performs an open-loop deployment sequence including ejection of the deputies and impulsive maneuvers that establishes an initial formation. After ejection from the mothership, each deputy passively drifts for a specified time to allow the required commissioning operations before a control law is engaged to acquire the desired formation and counteract any errors introduced during deployment. If necessary, the formation is reconfigured after control capability is established before nominal mission operations begin.

At present, most literature on spacecraft swarms only addresses the reconfiguration and formation-keeping problems. Instead, the primary objective of this paper is to provide safe deployment and formation acquisition procedures for spacecraft swarms in LEO subject to control errors and operational constraints. In particular, these procedures are developed to establish each of two formation classes recently proposed by the authors.[7] The key findings on formation design, guidance, and control from the authors' prior work are reviewed in the following.

Swarm Formation Design

The swarm formations proposed by the authors are defined using ROE, which are a slowly-varying state whose components are defined as explicit functions of the Keplerian orbit elements of a pair of spacecraft. This paper adopts the quasi-nonsingular ROE defined by D'Amico.[17] Using this definition, the ROE of the jth deputy with respect to the mothership $\delta\boldsymbol{\alpha}_j$ are given by

$$\delta\boldsymbol{\alpha}_j = \begin{pmatrix} \delta a_j \\ \delta\lambda_j \\ \delta e_{x,\,j} \\ \delta e_{y,\,j} \\ \delta i_{x,\,j} \\ \delta i_{y,\,j} \end{pmatrix} = \begin{pmatrix} \delta a_j \\ \delta\lambda_j \\ \delta e_j\cos(\theta_j) \\ \delta e_j\sin(\theta_j) \\ \delta i_j\cos(\varphi_j) \\ \delta i_j\sin(\varphi_j) \end{pmatrix} = \begin{pmatrix} (a_j - a_m)/a_m \\ (M_j - M_m) + (\omega_j - \omega_m) + \cos(i_m)(\Omega_j - \Omega_m) \\ e_j\cos(\omega_j) - e_m\cos(\omega_m) \\ e_j\sin(\omega_j) - e_m\sin(\omega_m) \\ i_j - i_m \\ \sin(i_m)(\Omega_j - \Omega_m) \end{pmatrix} \tag{1}$$

where a, e, i, Ω, ω, and M are the Keplerian orbit elements. The orbit elements of the mothership are denoted by the subscript m and those of the jth deputy are denoted by the subscript j. The ROE include the relative semimajor axis (δa), the relative mean longitude ($\delta\lambda$), the relative eccentricity vector (δe_x and δe_y), and the relative inclination vector (δi_x and δi_y). The quasi-nonsingular ROE are preferred over the singular or nonsingular as previously defined by the authors[18] because they are known to be equivalent to the integration constants of the Hill-Clohessey-Wiltshire equations to first order.[19]

Spacecraft formations are generally designed to satisfy two key constraints: 1) the passive relative motion should be bounded, and 2) the spacecraft must not collide. First, consider the bounded relative motion

requirement for spacecraft formations in LEO. The dominant perturbations in LEO are J_2 and differential atmospheric drag. Differential drag produces a relative acceleration in the (anti-)flight direction that causes secular drifts in the in-plane ROE (δa, $\delta\lambda$, δe_x, and δe_y).[18] The most significant effect of differential drag is a quadratic drift in $\delta\lambda$ due to the coupling of a linear drift in δa with Keplerian relative motion and J_2 earth oblateness effects. The drift in the relative eccentricity vector instead derives from the time variance of differential drag over the orbit due to either orbit eccentricity or the diurnal bulge. As such, the effect of differential drag on the relative eccentricity vector is smaller than the effect on the relative semimajor axis. For spacecraft formations in close proximity (separation on the order of km or less), the magnitude of the differential drag perturbation depends primarily on the differential ballistic properties of the spacecraft. As such, periodic control will be required to ensure bounded relative motion and/or collision avoidance unless the spacecraft are identical or the formation is deployed at sufficiently high altitude that the effects of atmospheric drag can be ignored. Instead, the effects of J_2 depend primarily on the geometry of the relative motion. A state transition matrix (STM) that includes the secular and long-period effects of J_2 on the mean ROE in near-circular orbits is given by

$$\delta\boldsymbol{\alpha}(t+\tau) = \boldsymbol{\Phi}^{J_2}(\boldsymbol{\alpha}_m,\tau)\delta\boldsymbol{\alpha}(t) = \begin{bmatrix} 1 & 0 & 0 & 0 & 0 & 0 \\ \Phi_{21}^{J_2} & 1 & 0 & 0 & \Phi_{25}^{J_2} & 0 \\ 0 & 0 & \cos(\dot{\omega}_m\tau) & -\sin(\dot{\omega}_m\tau) & 0 & 0 \\ 0 & 0 & \sin(\dot{\omega}_m\tau) & \cos(\dot{\omega}_m\tau) & 0 & 0 \\ 0 & 0 & 0 & 0 & 1 & 0 \\ \Phi_{61}^{J_2} & 0 & 0 & 0 & \Phi_{65}^{J_2} & 1 \end{bmatrix} \delta\boldsymbol{\alpha}(t) \tag{2}$$

where the following substitutions are used for clarity

$$\begin{gathered} \eta_m = \sqrt{1-e_m^2} \qquad \kappa_m = \frac{3}{4}\frac{J_2 R_E^2\sqrt{\mu}}{a_m^{7/2}\eta_m^4} \qquad \dot{\omega}_m = \kappa_m(5\cos^2(i_m)-1) \\ \Phi_{21}^{J_2} = -\left(\frac{3}{2}n_m + \frac{7}{2}\kappa_m(1+\eta_m)(3\cos^2(i_m)-1)\right)\tau \qquad \Phi_{25}^{J_2} = -\kappa_m(4+3\eta_m)\sin(2i_m)\tau \\ \Phi_{61}^{J_2} = \frac{7}{2}\kappa_m\sin(2i_m)\tau \qquad \Phi_{65}^{J_2} = 2\kappa_m\sin^2(i_m)\tau \end{gathered} \tag{3}$$

and n_m is the mean motion of the mothership. This model is obtained by simply neglecting the terms proportional to eccentricity in the STM recently derived by the authors for J_2-perturbed relative motion in arbitrarily eccentric orbits.[18] It is evident from the structure of this model that $\delta\lambda$ (second row of the STM) and δi_y (sixth row of the STM) will grow without bound if the mean δa or δi_x are nonzero. It follows that the necessary and sufficient condition to ensure bounded relative motion between all spacecraft in a swarm is that the mean δa and δi_x must be zero for all pairs of spacecraft. This means that all spacecraft must have the same mean semimajor axis and inclination. In light of this, subscripts are not included for the semi-major axis and mean motion in the following derivations to simplify notation.

A useful consequence of the use of the ROE state is that the constraints to ensure bounded relative motion fix only two of the six state elements. The remaining ROE ($\delta\lambda$, δe_x, δe_y, and δi_y) can be freely selected to ensure collision avoidance. In order to derive the required collision avoidance constraints, the known first order relationship between the ROE and the integration constants of the Hill-Clohessey-Wiltshire equations[19] is employed. Using this relationship, the relative position $\delta\boldsymbol{r}_j$ and relative velocity $\delta\boldsymbol{v}_j$ of the jth deputy with respect to the mothership are given by

$$\begin{pmatrix} \delta r_{R,\,j} \\ \delta r_{T,\,j} \\ \delta r_{N,\,j} \\ \delta v_{R,\,j} \\ \delta v_{T,\,j} \\ \delta v_{N,\,j} \end{pmatrix} = a \begin{bmatrix} 1 & 0 & -\cos(u_m) & -\sin(u_m) & 0 & 0 \\ 0 & 1 & 2\sin(u_m) & -2\cos(u_m) & 0 & 0 \\ 0 & 0 & 0 & 0 & \sin(u_m) & -\cos(u_m) \\ 0 & 0 & n\sin(u_m) & -n\cos(u_m) & 0 & 0 \\ -\frac{3}{2}n & 0 & 2n\cos(u_m) & 2n\sin(u_m) & 0 & 0 \\ 0 & 0 & 0 & 0 & n\cos(u_m) & n\sin(u_m) \end{bmatrix} \begin{pmatrix} \delta a_j \\ \delta\lambda_j \\ \delta e_{x,\,j} \\ \delta e_{y,\,j} \\ \delta i_{x,\,j} \\ \delta i_{y,\,j} \end{pmatrix} \tag{4}$$

where $u_m = M_m + \omega_m$ is the mean argument of latitude of the mothership, and the subscripts R, T, and N denote components in the radial, along-track, and cross-track directions, respectively. The radial direction is

aligned with the vector from the center of the earth to the mothership spacecraft, the cross-track direction is aligned with the angular momentum vector of the mothership orbit, and the along-track direction completes the right-handed triad. It should be noted that the relationship in Equation (4) holds and is more accurate for cylindrical and curvilinear coordinates.[20] However, the rectilinear model simplifies the computation of minimum separation distances and the modeling errors can reasonably be neglected for the inter-spacecraft separation distances considered in this work. Collision avoidance is ensured if the relative position vector is not smaller than a user-specified safe minimum value ϵ for all u_m. The authors have identified two classes of swarm formation that meet this requirement: an in-plane formation that ensures all spacecraft are separated in the orbit plane and an e/i vector separation formation that ensures separation in the plane perpendicular to the flight direction. The governing constraints for these formations are reviewed in the following.

First, consider an in-plane swarm formation. Since δa must be zero to ensure bounded relative motion, the in-plane separation between each pair of spacecraft is governed by $\delta\lambda$ and δe. Specifically, two spacecraft will have a minimum separation of ϵ in the orbit plane if $\delta\lambda$ satisfies

$$a|\delta\lambda| \geq 2a\delta e + \epsilon \quad \text{or} \quad a|\delta\lambda| \leq f(a, \delta e, \epsilon) \tag{5}$$

where the function f is given by

$$f(a, \delta e, \epsilon) = \begin{Bmatrix} \sqrt{3(a^2\delta e^2 - \epsilon^2)} & \text{if} & \epsilon \leq a\delta e < 2\epsilon \\ 2a\delta e - \epsilon & \text{if} & a\delta e \geq 2\epsilon \end{Bmatrix} \tag{6}$$

The primary consequence of the constraint in Equation (5) is that $|\delta\lambda|$ cannot be close to $2\delta e$. This constraint can be easily generalized to ensure collision avoidance between all spacecraft in a swarm as demonstrated in the following. Let $\delta\lambda_{jk}$ and δe_{jk} denote the relative mean longitude and the magnitude of the relative eccentricity vector, respectively, between the jth and kth deputies. To ensure safe motion for the entire swarm, it is sufficient to impose constraints on the ROE for each deputy such that Equation (5) is satisfied for all $\delta\lambda_{jk}$ and δe_{jk}. Next, suppose that the relative eccentricity vectors of all deputies are arranged in a pattern such that the minimum separation between any pair of deputies including uncertainty is δe_{min}. Finally, suppose that all $\delta\lambda_j$ with respect to the mothership are constrained by

$$a|\delta\lambda_j| \leq \frac{f(a, \delta e_{min}, \epsilon)}{2} \tag{7}$$

It is evident from this equation that the maximum difference between any two $a\delta\lambda_j$ is $f(a, \delta e_{min}, \epsilon)$. Because f monotonically increases with δe and all spacecraft are separated in relative eccentricity vector space by at least δe_{min}, then any two $\delta\lambda_j$ that satisfy Equation (7) must also satisfy Equation (5). Thus, all spacecraft in the swarm will be separated by at least ϵ at all times. Additionally, the constraint in Equation (7) only needs to be checked once for each deputy, allowing safety of the swarm to be verified at a computational cost that increases only linearly with the number of spacecraft. An example swarm of this type is illustrated in Figure 1. The relative motion in the RT-plane is shown in the left plot and the in-plane ROE are shown in the middle and right plots. In this example, ϵ is 100 m (shown in red) and the relative eccentricity vectors of the deputies are arranged such that $a\delta e_{min}$ is 200 m. The green region illustrates the acceptable range of $a\delta\lambda$, which is $\pm$150 m according to Equation (7). It can be seen that there are two deputies at opposite ends of this region. These correspond to the closest pair of deputies in the left plot, which are still separated by 100 m.

However, all of the deputy spacecraft encircle the mothership in the described configuration. It follows that a failure on one of the deputies may put the mothership at risk. This issue can be alleviated by simply defining all $\delta\lambda_j$ with respect to a virtual reference orbit that is offset in the flight direction from the mothership. To ensure the safety of the mothership, the offset must be large enough to satisfy Equation (5) for the largest δe_j.

While this swarm design allows a large number of spacecraft to operate in close proximity, the cost of this property is that the collision avoidance constraints are functions of $\delta\lambda$. Maneuver execution errors and differential drag cause drifts in $\delta\lambda$, which will have to be corrected by frequent maneuvers to ensure collision avoidance. It is therefore evident that a formation that ensures collision avoidance for arbitrary $\delta\lambda$ would substantially reduce actuation requirements on the spacecraft. For binary formations, D'Amico's e/i vector

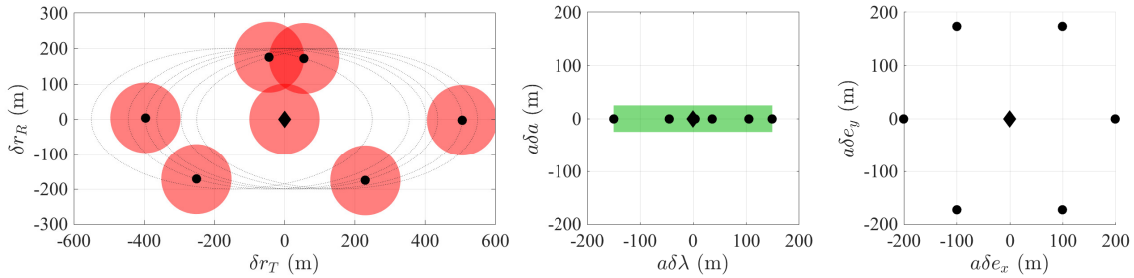

Figure 1. Example in-plane swarm formation including relative motion in the RT-plane (left) and the ROE (middle and right). Regions in the RT-plane with insufficient separation from at least one spacecraft (< 100 m) are shown in red and the range of $\delta\lambda$ that satisfies Equation (7) is shown in green.

separation concept[16] provides a means of ensuring a user-specified minimum separation in the plane perpendicular to the flight direction by constraining the relative eccentricity and inclination vectors. This concept has since been generalized to accommodate a large number of spacecraft.[7] Specifically, if δa and δi_x are both zero to provide passively bounded relative motion in J_2-perturbed orbits, the necessary and sufficient condition to ensure a minimum separation of ϵ between two spacecraft in the RN-plane is given by

$$\delta e_y^2 \geq \left(\frac{a^2 \delta i_y^2}{\epsilon^2} - 1 \right)^{-1} \delta e_x^2 + \frac{\epsilon^2}{a^2} \tag{8}$$

This constraint defines a hyperbola in relative eccentricity vector space for given δi_y and ϵ. This constraint can also be formulated in polar coordinates as

$$|\cos(\theta)| \leq \sqrt{\left(1 - \frac{\epsilon^2}{a^2 \delta e^2}\right)\left(1 - \frac{\epsilon^2}{a^2 \delta i^2}\right)} \quad \text{or} \quad |\sin(\theta)| \geq \frac{\epsilon}{a \delta e \delta i} \sqrt{\delta e^2 + \delta i^2 - \frac{\epsilon^2}{a^2}} \tag{9}$$

where θ is the phase angle of the relative eccentricity vector. This constraint can only be satisfied if both δe and δi are at least ϵ/a. Additionally, if this constraint is satisfied for some $\delta\boldsymbol{\alpha}$, then it will also be satisfied if $\delta\boldsymbol{\alpha}$ is multiplied by any constant of magnitude greater than or equal to one. Using this property, a passively safe swarm formation can be designed as follows. Suppose that the nominal relative eccentricity and inclination vectors of the jth deputy are given by

$$\delta \boldsymbol{e}_j = X_j \delta e_{sep} \begin{pmatrix} \cos(\theta) \\ \sin(\theta) \end{pmatrix} \qquad \delta \boldsymbol{i}_j = Y_j \delta i_{sep} \begin{pmatrix} 0 \\ 1 \end{pmatrix} \tag{10}$$

where X_j and Y_j are unique integers for each deputy and δe_{sep}, δi_{sep}, and θ are constant for the entire swarm. A minimum RN-plane separation of ϵ is guaranteed between all spacecraft in the swarm if the constraint in Equation (9) is satisfied for δe_{sep}, δi_{sep}, and θ. An example swarm of this type is illustrated in Figure 2. The relative motion in the RN-plane is shown in the left plot, the relative eccentricity vectors are shown in the middle plot, and the relative inclination vectors are shown in the right plot. In this example, ϵ is 100 m (shown in red) and $a\delta e_{sep}$ and $a\delta i_{sep}$ are both 200 m. From Equation (9), the minimum RN-plane separation is sufficient when θ is between 41^o and 139^o. Indeed, it can be seen that the relative eccentricity vectors have a phase angle of 41^o and each deputy is outside the circles defining the regions of insufficient separation from adjacent deputies at the point of closest approach. This means that all spacecraft are separated by at least 100 m at all times.

It is also possible to analytically ensure that a specified minimum separation is achieved including uncertainty. Suppose that it is known that separations between adjacent deputies in the presence of uncertainty can be as small as δe_{min} and δi_{min}. Additionally, suppose that these errors can also change the angle between

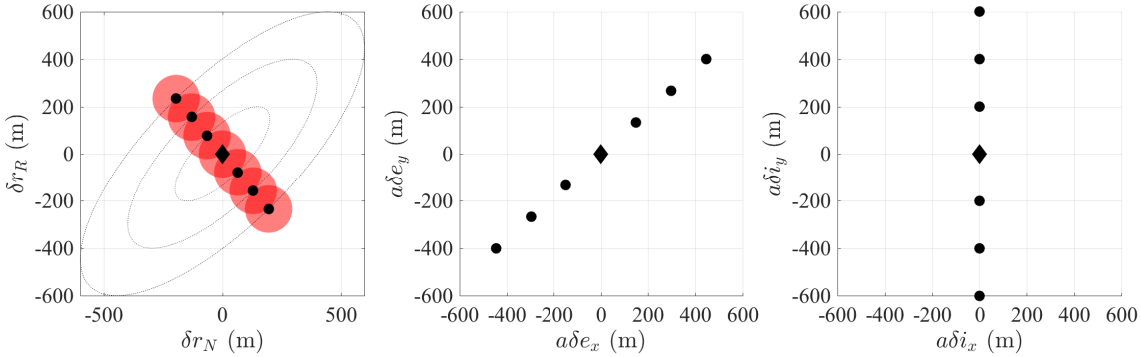

Figure 2. Example e/i vector separation swarm formation including relative motion in the RN-plane (left) and ROE (middle and right). Regions with insufficient separation from at least one spacecraft (< 100 m) are shown in red.

the relative eccentricity and inclination vectors of adjacent deputies by as much as ψ. A sufficient condition to ensure a minimum separation of ϵ between all spacecraft in the presence of these uncertainties is obtained by using δe_{min} and δi_{min} in Equation (9) and adding an offset of ψ to θ. The resulting constraint including uncertainty is given by

$$|\sin(\theta - \text{sign}(\tan(\theta))\psi)| \geq \frac{\epsilon}{a\delta e_{min}\delta i_{min}}\sqrt{\delta e_{min}^2 + \delta i_{min}^2 - \frac{\epsilon^2}{a^2}} \tag{11}$$

where the $\text{sign}(\tan(\theta))$ term ensures that ψ is applied in the worst-case direction.

One of the main benefits of this formation design is that the swarm can be allowed to freely drift as long as the phase angle of the relative eccentricity vectors satisfies Equation (11). However, it is evident from the dynamics model in Equation (2) that the relative eccentricity vector of each deputy passively rotates due to J_2. Thus, this constraint will be violated twice per precession period of the argument of perigee when the relative eccentricity vectors are nearly horizontal. With this in mind, Equation (11) provides a means of determining how long the swarm can be allowed to passively drift before actuation is required to establish safe separation in the RT-plane. Additionally, this constraint can be used to determine the required spacing between deputies to ensure sufficient RN-plane separation for specified θ and error parameters. Finally, using the same technique as employed for the in-plane formation, it is possible to verify the safety of the relative swarm at a computation cost that scales linearly with the number of spacecraft. This is accomplished by simply ensuring that the difference between the true relative eccentricity and inclination vectors of each deputy are within a prescribed envelope of their nominal values as defined in Equation (10).

Swarm Control

As demonstrated in the previous section, the relative inclination vectors of all spacecraft in the described formations are stable in orbits perturbed by both J_2 and differential drag. However, differential drag produces secular drifts in all of the in-plane ROE that must be periodically corrected to ensure safe and bounded relative motion. The control architecture presented in the following is derived under the assumption that the guidance profile follows the passive rotation of the relative eccentricity vector due to J_2 described in Equation (2) and is stationary in the other ROE. Thus, actuation is only required to counteract the effects of differential drag during nominal mission operations. To understand how this can be accomplished, it is first necessary to establish a model of the relationship between performed maneuvers and their effects on the ROE. Using D'Amico's control matrix $\mathbf{\Gamma}$ for near-circular orbits,[17] the time derivatives of the ROE corresponding to a

relative acceleration $\delta \boldsymbol{p}_j$ in the RTN frame applied to the jth deputy are given by

$$\delta \dot{\boldsymbol{\alpha}}_j = \boldsymbol{\Gamma}(\boldsymbol{\alpha}_m)\delta \boldsymbol{p}_j \qquad \boldsymbol{\Gamma}(\boldsymbol{\alpha}_m) = \frac{1}{an}\begin{bmatrix} 0 & 2 & 0 \\ -2 & 0 & 0 \\ \sin(u_m) & 2\cos(u_m) & 0 \\ -\cos(u_m) & 2\sin(u_m) & 0 \\ 0 & 0 & \cos(u_m) \\ 0 & 0 & \sin(u_m) \end{bmatrix} \tag{12}$$

It should be noted that while this model is derived for osculating orbits, it is also applicable to mean orbits because the magnitude of the short-period oscillations of a and u_m are small relative to their nominal values. The properties of this model can be used to simplify the control design problem. Specifically, it is evident from Equation (12) that along-track maneuvers provide the most efficient means of controlling the relative semimajor axis and relative eccentricity vector. Additionally, a change in $\delta\lambda$ can be efficiently generated by performing a pair of equal and opposite along-track maneuvers separated by a reasonable time (≥ 0.25 orbits). It follows that all of the in-plane ROE can be efficiently controlled using only along-track maneuvers, which can be realized using low-thrust or differential drag control. The authors have derived nonlinear bang-off-bang state space control laws for both of these actuation techniques that efficiently control all of the in-plane ROE using an approach inspired by recent work in impulsive formation reconfiguration.[21,22] These control laws can be employed to counteract errors introduced during the deployment sequence without modification. However, only the low-thrust control law is included in this paper for brevity.

The control law is designed to ensure that the in-plane ROE follow their prescribed guidance profile. Because the main function of the control law is to counteract differential drag, which primarily affects $\delta\lambda$, efficient control can be achieved by using a two-step process to compute the commanded acceleration. First, an initial estimate is computed based on current estimates of δa and $\delta\lambda$. Second, the acceleration command is computed by modulating the estimate to ensure that all executed maneuvers have a favorable effect on the relative eccentricity vector. Let the errors in relative mean longitude $\delta\lambda_{err}$ and the relative eccentricity vector $\delta \boldsymbol{e}_{err}$ for the jth deputy be defined as

$$\delta\lambda_{err} = \delta\lambda_j - \delta\lambda_{j,\,des} \qquad \delta \boldsymbol{e}_{err} = \begin{pmatrix} \delta e_{x,\,j} - \delta e_{x,\,j,\,des} \\ \delta e_{y,\,j} - \delta e_{y,\,j,\,des} \end{pmatrix} \tag{13}$$

where $\delta\lambda_{j,\,des}$, $\delta e_{x,\,j,\,des}$, and $\delta e_{y,\,j\,des}$ are the desired values from the guidance profile. The preliminary acceleration command $U^{com}_{\delta a,\delta\lambda_{err}}$ is given by

$$U^{com}_{\delta a,\delta\lambda_{err}}(\delta a, \delta\lambda_{err}) = \begin{Bmatrix} U & \text{if} & \delta\lambda_{err} \geq \Lambda^+(\delta a) \\ -U & \text{if} & \delta\lambda_{err} \leq \Lambda^-(\delta a) \\ 0 & & \text{otherwise} \end{Bmatrix} \tag{14}$$

where U is the acceleration produced by the thrusters and Λ^+ and Λ^- are the switching lines for thrust in the flight and anti-flight directions, respectively. These switching lines are functions of δa, the orbit semimajor axis, and control parameters given by

$$\begin{aligned} \Lambda^+(\delta a) &= \begin{Bmatrix} \max(-\delta\lambda_{db} + \dfrac{3an^2}{8U^*}\delta a^2 + \delta\lambda_{wait}, \delta\lambda_{db}) & \text{if} & \delta a \geq 0 \\ \delta\lambda_{db} - \dfrac{3an^2}{8U^*}\delta a^2 & \text{if} & \delta a < 0 \end{Bmatrix} \\ \Lambda^-(\delta a) &= \begin{Bmatrix} -\delta\lambda_{db} + \dfrac{3an^2}{8U^*}\delta a^2 & \text{if} & \delta a \geq 0 \\ \min(\delta\lambda_{db} - \dfrac{3an^2}{8U^*}\delta a^2 - \delta\lambda_{wait}, -\delta\lambda_{db}) & \text{if} & \delta a < 0 \end{Bmatrix} \end{aligned} \tag{15}$$

where $\delta\lambda_{db}$ is the size of the deadband, U^* is the maximum time-averaged thrust that is guaranteed to be compatible with the modulation produced by the relative eccentricity vector control law, and $\delta\lambda_{wait}$ is the

change in $\delta\lambda$ due to the drift between maneuvers, which is given by

$$\delta\lambda_{wait} = \frac{3}{2}|\delta a| \max\left(\Delta t_{rec} - \frac{an}{U^*}|\delta a|, 0\right) \tag{16}$$

The drift is computed such that $\delta\lambda_{err}$ will be within the deadband within a specified reconfiguration time Δt_{rec}. Next, it is necessary to modulate $U^{com}_{\delta a,\delta\lambda_{err}}$ to ensure that executed maneuvers reduce the magnitude of $\delta\boldsymbol{e}_{err}$. It is evident from the structure of the control matrix in Equation (12) that the phase angle of the change in the relative eccentricity vector produced by an along-track maneuver is a function of the location of the maneuver. With this in mind, control of the relative eccentricity vector is achieved as follows. If the magnitude of $||\delta\boldsymbol{e}_{err}||_2$ is within a specified deadband δe_{db}, then the commanded acceleration is equal to $U^{com}_{\delta a,\delta\lambda_{err}}$. However, if $||\delta\boldsymbol{e}_{err}||_2$ is larger than the deadband, the commanded acceleration is zero unless the resulting maneuver will decrease $||\delta\boldsymbol{e}_{err}||_2$. Using this control logic, the commanded acceleration U^{com} is given by

$$U^{com} = \begin{Bmatrix} U^{com}_{\delta a,\delta\lambda_{err}} & \text{if} & ||\delta\boldsymbol{e}_{err}||_2 <= \delta e_{db} \\ U^{com}_{\delta a,\delta\lambda_{err}} & \text{if} & -\dfrac{\text{sign}(U^{com}_{\delta a,\delta\lambda_{err}})\delta\boldsymbol{e}_{err}}{||\delta\boldsymbol{e}_{err}||_2} \cdot \begin{pmatrix}\cos(u_m)\\ \sin(u_m)\end{pmatrix} \geq \cos(\zeta) \\ 0 & & \text{otherwise} \end{Bmatrix} \tag{17}$$

where the angle $\zeta \leq \pi/2$ is selected to control how fast $||\delta\boldsymbol{e}_{err}||_2$ must decrease and is constant for the entire swarm. Because this control law allows maneuvers that increase $||\delta\boldsymbol{e}_{err}||_2$ up to δe_{db}, it is evident that this approach allows a limit cycle in which the relative eccentricity vector traces a circle of radius δe_{db} about $\delta\boldsymbol{e}_{des}$. Additionally, it is necessary to ensure that the deputies can follow the switching lines defined in Equation (15) to prevent $\delta\lambda_{err}$ from overshooting the deadband. Specifically, it is necessary to select U^* so that it is no larger than the average of U^{com} over one orbit. This parameter is defined by considering the limiting cases of the relative eccentricity vector control law. If $||\delta\boldsymbol{e}_{err}||_2$ is larger than the deadband, then the control law allows maneuvers that span at least ζ/π of the orbit. On the other hand, if $||\delta\boldsymbol{e}_{err}||_2$ is within the deadband, then the resulting maneuvers can trace out a path no longer than $2\pi\delta e_{db}$ in relative eccentricity vector space in one orbit. From Equation (12), this corresponds to an average acceleration of $an^2\delta e_{db}/2$. Using these results, U^* will be no larger than the average of U^{com} over one orbit if it is defined as

$$U^* = \min\left(\frac{\zeta}{\pi}U, \frac{1}{2}an^2\delta e_{db}\right) \tag{18}$$

From this equation it is evident that U^* can be no larger than half of U. Additionally, U^* may be constrained if $a\delta e_{db}$ is small, corresponding to a precise control requirement. However, if micronewton low thrust control is used in LEO ($n \approx 1 \times 10^{-3}$), then the deadband will not be the limiting factor for U^* unless $a\delta e_{db}$ is on the order of a few meters or less.

DEPLOYMENT AND FORMATION ACQUISITION

The formation designs and low-thrust control law reviewed in the previous section provide a means of ensuring safe and bounded relative motion between a large number of spacecraft. It is now necessary to develop procedures that safely initialize these formations that are robust to control errors and accommodate operational constraints. To meet this need, this paper provides deployment and formation acquisition procedures for both in-plane and e/i vector separation formations. Specifically, an open-loop command sequence for the mothership is developed for each of these formations that allows a large number of deputies to be safely deployed into a passively safe formation with minimal drift between spacecraft. After a commissioning phase of specified duration, the aforementioned low-thrust control law is engaged for each deputy to counteract any errors introduced during the deployment sequence. For each formation, the open-loop deployment sequence is first presented without control errors for clarity. Next, control errors are introduced and used to derive analytical lower bounds on the duration of the passively safe relative motion after the deployment sequence. These bounds are used to specify error requirements for the deployment system and specify the duration of the commissioning phase for the deputies.

In-Plane Formation Deployment

In order to ensure a specified minimum separation in the orbit plane between all spacecraft in a swarm, it is sufficient to satisfy two conditions: 1) the relative eccentricity vectors of all spacecraft must have a sufficient minimum spacing, and 2) the relative mean longitudes of all deputies must be close together. This is accomplished using the deployment procedure described in the following. Suppose that each deputy is ejected from the mothership using a device such as the P-POD CubeSat deployer.[23] Let the relative velocity $\Delta\mathbf{v}_{eject}$ in the RTN frame be given by

$$\Delta\mathbf{v}_{eject} = -\Delta\mathrm{v}_{eject}\begin{pmatrix}\cos(\gamma)\\ \sin(\gamma)\\ 0\end{pmatrix} \tag{19}$$

where $\Delta\mathrm{v}_{eject}$ is the magnitude of the ejection velocity and γ is the angle between the ejection velocity vector and the radial direction. The negative sign is included so that the $\delta\lambda$ and subsequent drift caused by the ejection are both positive, but the procedure is equally valid when the deputies are ejected in the opposite direction. Using this convention, a γ of 0^o corresponds to an ejection in the -R direction and a γ of 90^o corresponds to an ejection in the -T direction. From the control matrix in Equation (12), the ROE of the deputy with respect to the mothership immediately after ejection $\delta\boldsymbol{\alpha}_{eject}$ are given by

$$\begin{pmatrix}\delta a_{eject}\\ \delta\lambda_{eject}\\ \delta e_{x,\,eject}\\ \delta e_{y,\,eject}\end{pmatrix} = \frac{\Delta\mathrm{v}_{eject}}{an}\begin{pmatrix}-2\sin(\gamma)\\ 2\cos(\gamma)\\ -\cos(\gamma)\sin(u_m) - 2\sin(\gamma)\cos(u_m)\\ \cos(\gamma)\cos(u_m) - 2\sin(\gamma)\sin(u_m)\end{pmatrix} \tag{20}$$

It will be demonstrated in the following analysis that γ must be small in order to ensure that the minimum separation constraint is satisfied, resulting in an ejection velocity vector closely aligned with the radial direction. Thus, Equation (20) can be simplified using a set of small angle approximations given by

$$\cos(\gamma) = \cos(2\gamma) = 1 \qquad 2\sin(\gamma) = \sin(2\gamma) \tag{21}$$

Substituting the expressions in Equation (21) into Equation (20) and simplifying the result yields

$$\begin{pmatrix}\delta a_{eject}\\ \delta\lambda_{eject}\\ \delta e_{x,\,eject}\\ \delta e_{y,\,eject}\end{pmatrix} = \frac{\Delta\mathrm{v}_{eject}}{an}\begin{pmatrix}-\sin(2\gamma)\\ 2\\ -\sin(u_m + 2\gamma)\\ \cos(u_m + 2\gamma)\end{pmatrix} \tag{22}$$

It is clear from this expression that the magnitudes of all of the ROE scale with the ejection velocity. However, the ejection angle only has an effect on the relative semimajor axis and the phase angle of the relative eccentricity vector.

A key constraint on the deployment parameters is that an ejected deputy must not collide with the mothership. If the ejection angle is set to zero, then δa_{eject} will also be zero, which means that the ejected deputy will exhibit a periodic trajectory with respect to the mothership. It follows that the deputy will collide with the mothership after one orbit. In order to ensure that the separation between the deputy and mothership is at least ϵ after the ejection, consider the following model. From the relationship between the ROE and the relative motion described in Equation (4), the in-plane relative motion of two spacecraft will have a minimum separation of ϵ if $|\delta\lambda| \geq 2\delta e + \epsilon/a$. From the initial ROE after the ejection maneuver in Equation (22), it is possible to ensure that a safe formation is achieved after one orbit if δa_{eject} is large enough to cause $|\delta\lambda|$ to increase by ϵ/a. Neglecting the effects of J_2 in Equation (2), the drift rate of $\delta\lambda$ is related to δa by

$$\delta\dot{\lambda} = -1.5n\delta a \tag{23}$$

If follows that $\delta\lambda$ will increase by ϵ/a over one orbit if δa_{eject} satisfies

$$\delta a_{eject} \leq -\frac{\epsilon}{3\pi a} \tag{24}$$

Substituting the expression for δa_{eject} in Equation (22) and solving for γ yields

$$\gamma \geq \frac{1}{2} \arcsin\left(\frac{n\epsilon}{3\pi \Delta \mathrm{v}_{eject}}\right) \tag{25}$$

Thus, the minimum ejection angle that provides a specified minimum separation of an ejected deputy from the mothership is a function of the orbit mean motion, the specified minimum separation, and the ejection velocity. However, it should be noted that the collision avoidance requirement in Equation (7) requires all $\delta\lambda_j$ to be close together. Thus, it is also desirable to minimize δa_{eject} so that the deputies do not drift apart over the deployment sequence. It follows that the ideal choice of γ is the smallest value that satisfies the constraint in Equation (25). With this in mind, it is worthwhile to consider the magnitudes of the variables that govern the selection of γ. The mean motion is known to be approximately 1×10^{-3} in LEO and the ejection velocity produced by CubeSat deployers is generally on the order of 1 m/s. Using these values, if ϵ is less than one kilometer, than γ will be no larger than 3.3^o according to Equation (25), validating the employed small angle approximations. It should also be noted that it is possible to select a negative γ that results in an opposite drift that satisfies Equation (5) after one orbit. However, in this case there would still be a chance of the deputy colliding with the mothership when the total drift of $\delta\lambda$ since ejection is near $4\delta e_{eject}$. In such a scenario, failure of a single deputy would put the mothership at risk. Thus, positive γ are preferred to ensure the safety of the mothership in the event of a deputy malfunction. Accordingly, the preferred ejection direction is primarily aligned in the -R direction with a small component in the -T direction. Finally, it is necessary to specify the timing of the deputy ejections. It is evident from Equation (22) that the relative eccentricity vector produced by an ejection maneuver will lie on a circle of radius $\Delta \mathrm{v}_{eject}/(an)$. Additionally, it is desirable to maximize the separation in relative eccentricity vector space between any pair of deputies. This can be accomplished by evenly spacing the relative eccentricity vectors of the deputies along the circle, which corresponds to evenly spacing the ejections over one orbit. From simple trigonometry, the separation between adjacent deputies in relative eccentricity vector space is given by

$$\delta e_{sep} = 2\frac{\Delta \mathrm{v}_{eject}}{an} \sin\left(\frac{\pi}{N}\right) \tag{26}$$

The described deployment sequence for a swarm with nine deputies in LEO is illustrated in Figure 3. The RT-plane trajectory for the first orbit for all of the deputies with respect to the mothership is shown in the left plot and the ROE at the end of the first orbit are shown in the middle and right plots. In this example, the required minimum separation between all spacecraft is 200 m (shown in red). The mothership ejects each of nine deputies at 0.5 m/s with an ejection angle of 1.4^o in order to ensure safe separation from the mothership after one orbit. Indeed, it can be seen in the left plot that the first ejected deputy is 200 m away from the mothership after one orbit. Also, because all $a\delta\lambda_{jk}$ are no larger than 200 m (see middle plot) and all $a\delta e_{jk}$ are at least 300 m (see right plot), Equation (5) must be satisfied for all pairs of deputies for an ϵ of 200 m. In particular, the minimum separation between any pair of deputies from the left plot is approximately 250 m. Additionally, the deputies do not drift relative to each other after ejection because all of them have the same semimajor axis. However, all of the deputies have a nonzero relative semimajor axis with respect to the mothership, meaning that the deputies will continue to drift away from the mothership unless corrective action is taken. The drift of the swarm can be arrested by having the mothership perform two equal maneuvers in the anti-flight direction separated by half of an orbit. These maneuvers will eliminate the relative semimajor axis between the mothership and deputies produced by the ejection without affecting the relative eccentricity vectors of the deputies.[22] The total delta-v cost of both maneuvers is equal to the along-track component of the ejection velocity in Equation (19).

In order to use such a deployment sequence in a real mission, it is necessary to account for ejection and maneuver execution errors, which will limit the duration of the passively safe relative motion. Let the ejection velocity vector including errors be given by

$$\Delta \mathbf{v}_{eject} = -(1 + \sigma_{eject})\Delta \mathrm{v}_{eject} \begin{pmatrix} \cos(\gamma + \sigma_\gamma) \\ \sin(\gamma + \sigma_\gamma) \\ 0 \end{pmatrix} \tag{27}$$

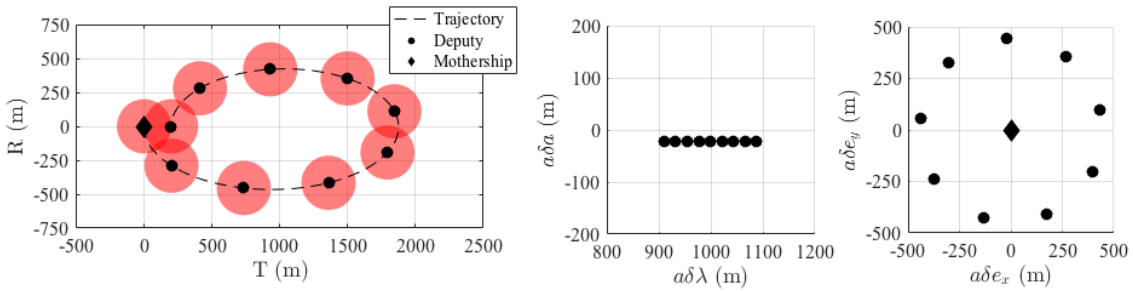

Figure 3. RT-plane trajectory (left) and ROE (right) for in-plane formation after ejection from mothership. Regions with insufficient separation from at least one spacecraft ($<$ 200 m) are shown in red.

where σ_{eject} is the ejection velocity error expressed as a fraction of the nominal velocity and σ_γ is the ejection angle error. This model captures the fact that errors for these ejections are largely due to two decoupled sources: the deployer mechanism (σ_{eject}) and the mothership attitude controller (σ_γ). Using the same small angle assumption used to derive Equation (22), the ROE produced by such an ejection are given by

$$\begin{pmatrix} \delta a_{eject} \\ \delta\lambda_{eject} \\ \delta e_{x,\,eject} \\ \delta e_{y,\,eject} \end{pmatrix} = \frac{(1+\sigma_{eject})\Delta \mathrm{v}_{eject}}{an} \begin{pmatrix} -\sin(2(\gamma+\sigma_\gamma)) \\ 2 \\ -\sin(u_m+2(\gamma+\sigma_\gamma)) \\ \cos(u_m+2(\gamma+\sigma_\gamma)) \end{pmatrix} \tag{28}$$

The ROE produced by such an ejection will be within the green region shown in Figure 4. It can be seen that the feasible region in δa and $\delta\lambda$ is a trapezoid and the feasible region for the relative eccentricity vector is a truncated sector. These ejection errors have four noteworthy effects on the deployment procedure. First, the ejection velocity and angle must be selected such that each deputy is safely separated from the mothership subject to worst-case errors. Second, the separation between adjacent deputies in relative eccentricity vector space will be reduced. Third, the ejection errors cause the initial values of $\delta\lambda$ to differ by as much as $\delta\lambda_{err}$. Fourth, the relative semimajor axis produced by the ejection will be between δa_{min} and δa_{max}. As a result, the relative semimajor axis between deputies can be as large as δa_{err}, which will cause the deputies to continue to drift apart after ejection from the mothership. The commissioning phase must end before this drift puts the spacecraft at risk of collision.

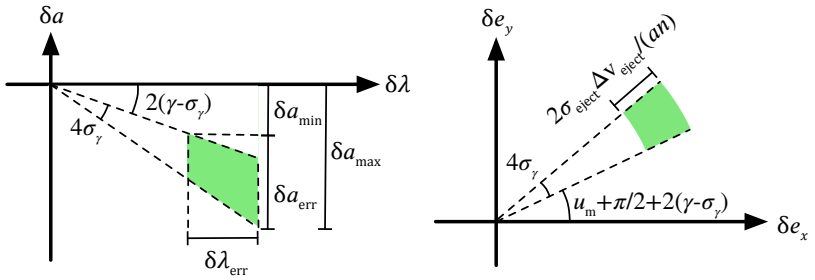

Figure 4. Possible ROE immediately after ejection including errors.

Using the model in Equation (28) it is possible to derive a closed-form expression for the earliest time after ejection when a pair of spacecraft may be at risk of collision. First, consider the effects of the ejection errors on the separation between deputies in relative eccentricity vector space. Using the worst-case magnitudes and

angular separations of two adjacent deputies in relative eccentricity vector space, the minimum separation is given by

$$\delta e_{min} = 2\sin(\pi/N - 2\sigma_\gamma)(1-\sigma_{eject})\frac{\Delta \mathrm{v}_{eject}}{an} \tag{29}$$

By comparing this expression with Equation (26), it is clear that the decrease in separation in relative eccentricity vector space scales directly with σ_{eject} and with the ratio σ_γ/N. Next consider the effect of the ejection errors on the relative semimajor axis. Specifically, the nominal ejection angle must be large enough to ensure safe separation from the mothership with the worst-case ejection errors. The minimum ejection angle that guarantees this condition is computed by setting δa_{eject} in Equation (28) equal to the required value to achieve a drift of ϵ over one orbit from Equation (24) and solving for γ, which yields

$$\gamma \geq \frac{1}{2}\arcsin\left(\frac{n\epsilon}{3\pi(1-\sigma_{eject})\Delta \mathrm{v}_{eject}}\right) + \sigma_\gamma \tag{30}$$

Using this angle, the smallest and largest values of the relative semimajor axis produced by an ejection, denoted δa_{min} and δa_{max}, respectively, are given by

$$\delta a_{min} = -\frac{\epsilon}{3\pi a} \qquad \delta a_{max} = -\sin(2(\gamma+\sigma_\gamma))(1+\sigma_{eject})\frac{\Delta \mathrm{v}_{eject}}{an} \tag{31}$$

Also, the largest δa and $\delta\lambda$ differences between deputies produced by these ejection errors, denoted δa_{err} and $\delta\lambda_{err}$, respectively, are given by

$$\delta a_{err} = |\delta a_{max} - \delta a_{min}| \qquad \delta\lambda_{err} = 4\sigma_{eject}\frac{\Delta \mathrm{v}_{eject}}{an} \tag{32}$$

Next, it is necessary to derive a lower bound on the duration of the passively safe relative motion after the deployment sequence. This is accomplished by first computing the largest possible separation in $\delta\lambda$ between two deputies as a function of time. The largest separation in $\delta\lambda$ between any pair of deputies is obtained if the first deputy is ejected with a relative semimajor axis of δa_{max} and the last deputy is ejected with a relative semimajor axis of δa_{min}. If t_1 denotes the ejection time of the first deputy, then the relative mean longitude of this deputy with respect to the mothership $\delta\lambda_1$ can be expressed as

$$\delta\lambda_1(t) = 2(1+\sigma_{eject})\frac{\Delta \mathrm{v}_{eject}}{an} - 1.5n\delta a_{max}(t-t_1) \tag{33}$$

Similarly, if t_N denotes the ejection time of the Nth deputy, then the relative mean longitude of this deputy with respect to the mothership $\delta\lambda_N$ is given by

$$\delta\lambda_N(t) = 2(1-\sigma_{eject})\frac{\Delta \mathrm{v}_{eject}}{an} - 1.5n\delta a_{min}(t-t_N) \tag{34}$$

Because the deployments are evenly spaced along a single orbit, the difference between t_N and t_1 can be no larger than $2\pi/n$. The worst-case relative mean longitude between two deputies $\delta\lambda_{wc}$ is obtained by taking the difference between Equations (33) and (34), which is given by

$$\delta\lambda_{wc}(t) = 3\pi|\delta a_{max}| + \delta\lambda_{err} + 1.5n|\delta a_{err}|(t-t_N) \tag{35}$$

Next, let the duration of the commissioning phase t_{com} be the same for every deputy. This value must be selected such that $\delta\lambda_{wc}$ satisfies Equation (5) using the smallest possible separation in relative eccentricity vector space for all $t - t_N \leq t_{com}$. This constraint is given by

$$t_{com} \leq \frac{f(a,\delta e_{min},\epsilon) - 3\pi|\delta a_{max}| - \delta\lambda_{err}}{1.5n|\delta a_{err}|} \tag{36}$$

This expression provides a closed-form bound on the allowable duration of the commissioning phase as a function of the number of spacecraft, the required separation from the mothership, and the ejection parameters. To illustrate the behavior of this function, the number of allowable orbits for the commissioning phase

is plotted against the ejection velocity and the ejection angle error in Figure 5 for swarms with 6 (left), 9 (middle), and 12 (right) deputies. These computations are performed for a σ_{eject} of 0.1 and ϵ of 125 m. The black region indicates configurations where t_{com} is less than one orbit and each of the contour lines indicates an increase of one orbit. It can be seen that t_{com} is no larger than 15 orbits (approximately 1 day) for all considered parameters. Thus, use of this formation acquisition procedure will require the deputies to be rapidly commissioned to ensure safe relative motion in the presence of ejection errors. Additionally, for ejection velocities of over 1 m/s, t_{com} is most sensitive to changes in σ_γ and N. The sensitivity to σ_γ is expected because t_{com} scales with the inverse of δa_{err}, which depends strongly on the ejection angle error. The sensitivity to N is due to the fact that separation in relative eccentricity vector space scales with $1/N$, so including more deputies results in tighter bounds on $\delta\lambda$.

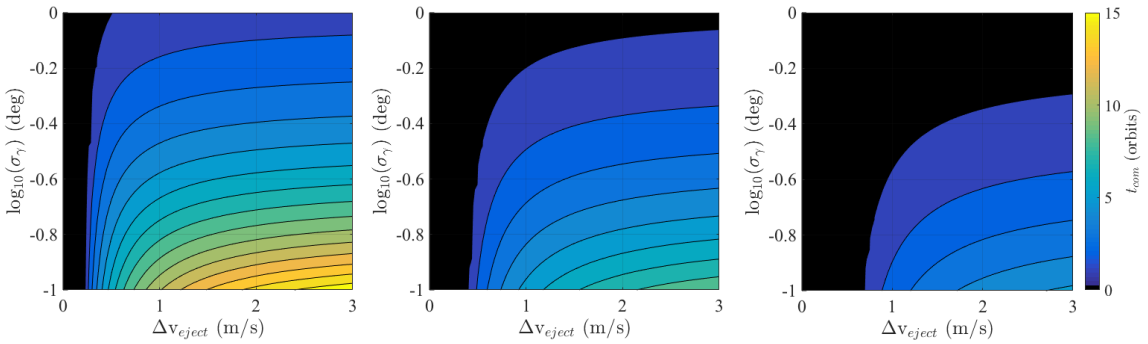

Figure 5. Maximum allowable commissioning phase duration as function of σ_γ and $\Delta\mathbf{v}_{eject}$ for a swarms of 6 (left), 9 (middle), and 12 (right) deputies.

Overall, the proposed deployment procedure provides a means of safely acquiring an in-plane swarm formation at low delta-v cost subject to operational constraints and control errors. The relationship between key deployment parameters and the maximum allowable duration of the commissioning phase is captured by the model in Equation (36). This model suggests that this deployment procedure is subject to three key limitations. First, sub-degree attitude control precision will be necessary for the mothership in order to provide the deputies with several orbits of commissioning time. Second, use of differential drag control to counteract errors introduced by this deployment procedure is not practical. The authors have found that several orbits of actuation time may be required to produce a sufficient change in δa to counteract these ejection errors using differential drag control,[7] reducing the allowed commissioning time to effectively zero. Third, the allowable duration of the commissioning phase depends on the number of deputies in the swarm. However, this limitation can be overcome by performing repeated deployments of small swarms ($\sim$5-10 deputies), which can later be reconfigured into a single larger swarm.

E/I Vector Separation Formation Acquisition

The main drawback of the proposed in-plane formation acquisition procedure is that the deputy spacecraft must be commissioned quickly to ensure collision avoidance. It is possible to substantially increase the duration of the safe relative motion after ejection by using an e/i vector separation formation. Because the minimum separation constraint in the RN-plane is not a function of $\delta\lambda$, the residual δa between deputies caused by ejection errors will not cause a collision risk. Instead, the minimum separation constraint is a function of the phase angle of the relative eccentricity vector, which precesses slowly due to J_2. It follows that proper selection of the initial formation can guarantee several days or more of passively safe relative motion even when ejection and maneuver execution errors are included.

A formation as described in Eq. (10) with positive and consecutive X_j and Y_j can be produced by repeating the open-loop command sequence described in the following. This command sequence is inspired by recent work in impulsive formation reconfiguration,[21,22] and produces the desired formation at minimum delta-

v cost. Specifically, Gaias demonstrated that the minimum delta-v formation reconfiguration problem is identical to a minimum length path planning problem in relative eccentricity and inclination vector spaces.[21] Using this result, the mothership performs a sequence of maneuvers that cause the relative eccentricity and inclination vectors of each deputy to approach their desired states in a straight line, minimizing the delta-v cost. For simplicity, it is assumed that the nominal ejection velocity of the deployer is $an\delta i_{sep}$. This ejection velocity is selected to eliminate the need for a cross-track maneuver to ensure separation from the mothership. The open-loop command sequence for the mothership that acquires the described formation consists of a four-step process that is repeated for each deputy. First, a deputy is ejected in the cross-track direction at one of the extreme latitudes ($u_m = 90^o$ or 270^o), which separates the deputy from the mothership in only δi_y according to the control model in Equation (12). This ejection maneuver produces a trajectory that evolves in a straight line in the RTN frame as described in Equation (4). Thus, the deputy will collide with the mothership in half of an orbit if no maneuvers are performed. In order to establish a passive separation from the deputy before this occurs, the mothership performs a maneuver with a magnitude of $an\delta e_{sep}/4$ in the (anti-)flight direction when $u_m = \theta$ or $\theta + 180^o$ to produce a change in the relative eccentricity vector in the desired direction. Next, the mothership performs a cross-track maneuver with a magnitude of $an\delta i_{sep}$ one half orbit after the ejection maneuver and in the same direction. This maneuver increases the separation from the previously ejected deputy in order to allow the next deputy to be safely deployed. Finally, the mothership performs another maneuver in the (anti-)flight direction that is equal in magnitude and opposite in direction to the first maneuver. This simultaneously increases the separation in relative eccentricity vector space to δe_{sep} and removes the difference in δa produced by the first maneuver. These command sequence is summarized in Table 1 and the evolution of the relative eccentricity and inclination vectors during of this sequence is illustrated in in Figure 6. This command sequence allows an arbitrary number of deputies to be deployed at

Table 1. Open-loop deployment command sequence for e/i vector separation formation.

#	Description	Location	Direction	Magnitude (m/s)	Sign
1	Deputy ejection	$u_1 = 90^o$ or 270^o	Cross-track	$an\delta i_{sep}$	sign(sin(u_1))
2	δe maneuver	$u_2 = \theta$ or $\theta + 180^o$	Flight	$an\delta e_{sep}/4$	-sign(cos($u_2 - \theta$))
3	δi maneuver	$u_3 = u_1 + 180^o$	Cross-track	$an\delta i_{sep}$	-sign(sin(u_3))
4	δe maneuver	$u_4 = u_2 + 180^o$	Flight	$an\delta e_{sep}/4$	-sign(cos($u_4 - \theta$))

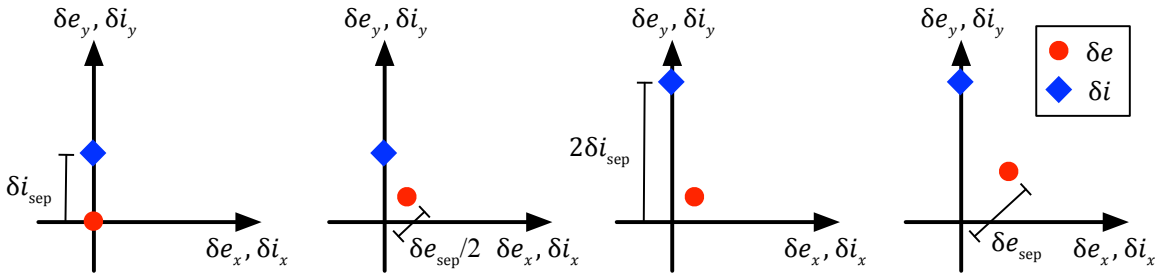

Figure 6. Evolution of relative eccentricity and inclination vectors of a deployed deputy in an e/i vector separation formation after ejection (left), after the first flight direction maneuver (middle left), after the cross-track maneuver (middle right) and after the second flight direction maneuver (right).

a rate of one per orbit. However, each command sequence will cause a change in $\delta\lambda$ due to the along-track maneuvers. Counteracting the cumulative change in $\delta\lambda$ when a large number of deputies are deployed may incur large delta-v costs. This issue can be mitigated by adding a half orbit delay between deputy ejections. This can be accomplished by ensuring that the selected value of u_1 is different for every deployed deputy using the convention in Table 1. This will reverse the locations and directions of all performed maneuvers, causing equal and opposite changes in $\delta\lambda$ each time the command sequence is executed. This approach will

reduce the delta-v cost of ensuring a safe separation in the RT-plane after the deputies are commissioned, but will require 50% more time to deploy all of the deputies. In either of these cases, the cross-track maneuver is not necessary after the last deputy is deployed because the ejection already produces a safe separation from the mothership and all other deputies. Thus, the total delta-v cost of the open-loop command sequence $\Delta \mathrm{v}_{tot}$ is given by

$$\Delta \mathrm{v}_{tot} = an((N-1)\delta i_{sep} + N\delta e_{sep}/2) \tag{37}$$

This delta-v cost is exactly equal to the lower-bound provided by Gaias to drive the first ejected deputy to its final state from an initial condition immediately following ejection from the mothership.

A limitation of the e/i vector separation formation is that the number of spacecraft scales linearly with the size of the swarm. Additionally, the previously described deployment sequence is subject to the constraint that all deputies must lie on a ray starting at the origin in the relative eccentricity and inclination vector spaces. This constraint is due to the fact that the mothership cannot approach a previously deployed deputy without compromising separation in the RN-plane. The number of spacecraft that can be deployed in a specified volume can be doubled by making a simple modification to the command sequence as described in the following and illustrated in Figure 7. Suppose that N is even and the desired formation has $N/2$ deputies on each side of the mothership as illustrated in Figure 2. To initialize this formation, the mothership first executes the open-loop command sequence in Table 1 $N/2$ times, omitting the final cross track maneuver. The relative eccentricity and inclination vectors of the deployed deputies after this sequence are shown in Figure 7 (left). Next, the mothership executes the three maneuvers described in Table 1 except that the magnitudes of the maneuvers in the flight direction are increased by a factor of $N/2$ and the magnitude of the cross-track maneuver is increased by a factor of $N/2-1$. As shown in Figure 7 (middle), these maneuvers increase the separation between the mothership and the deployed deputies. Finally, the open-loop command sequence is repeated for the remaining deputies, except that the directions of all maneuvers are reversed. This causes the mothership to approach the first set of deployed deputies in the relative eccentricity and inclination vector spaces while deploying the second set of deputies in the opposite direction as shown in Figure 7 (right). This approach doubles the number of deputies that can be deployed within a given range of the mothership, but increases the delta-v cost of the formation acquisition by 50% due to the additional maneuvers required to separate the mothership from the first set of deployed deputies.

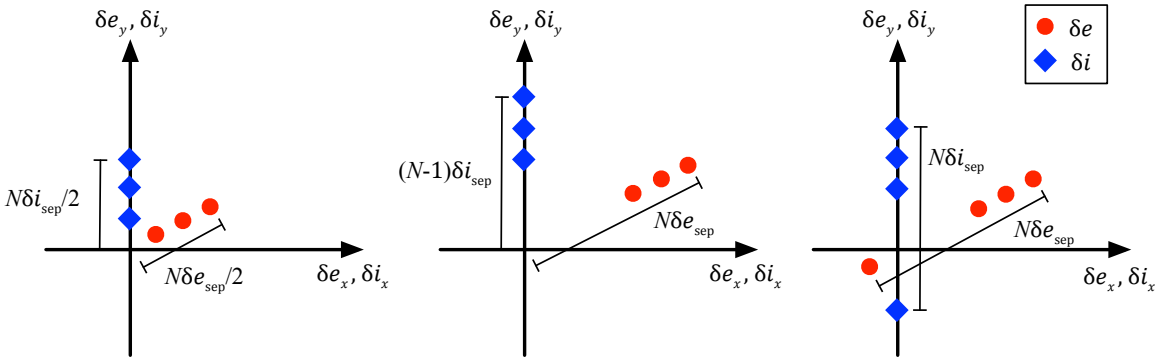

Figure 7. ROE after deployment of first half of deputies (left), after intermediate maneuver sequence (middle), and after deployment of first deputy from second set (right) in two-sided deployment sequence.

It is now necessary to model the effects of ejection and maneuver execution errors on the performance of this deployment procedure. Because the e/i vector separation formation provides a safe minimum separation in the RN-plane, the effects of ejection and maneuver execution errors on δa and $\delta\lambda$ have no impact on the safety of the formation. Additionally, if it is assumed that the deputy ejections and mothership maneuver directions are controlled with sub-degree precision, then the effects of along-track maneuvers on the relative inclination vector and the effects of cross-track maneuvers on the relative eccentricity vector will be on the

order of 1% or less. These effects are negligible when compared to reasonable ejection velocity and maneuver execution errors. Thus, the rotation of the relative eccentricity and inclination vectors between adjacent deputies due to maneuver execution errors can be reasonably neglected. It follows that the only significant effects of these errors are reductions in the spacing between the relative eccentricity and inclination vectors of adjacent deputies. With this in mind, consider the smallest possible separation between two deputies produced by the described deployment procedure. Let the ejection velocity error be denoted σ_{eject} as before and let the maneuver execution error be denoted σ_{man}. The separation in relative eccentricity vector space is minimized if the magnitudes of the maneuvers in the (anti-)flight direction are minimized. The separation in relative inclination vector space is minimized if one deputy ejection has the smallest possible velocity, the cross-track maneuver has the smallest possible delta-v, and the following deputy ejection has the highest possible velocity. In this case, the minimum separations between adjacent deputies in relative eccentricity and inclination vector spaces are given by

$$\delta e_{min} = (1 - \sigma_{man})\delta e_{sep} \qquad \delta i_{min} = (1 - 2\sigma_{eject} - \sigma_{man})\delta i_{sep} \tag{38}$$

For known error values, a minimum RN-plane separation of ϵ is guaranteed if θ satisfies Equation (11) for $\psi = 0$ with these minimum separations. These relations also provide a means of computing the maximum allowable duration of the commissioning phase. Suppose Equation (11) is satisfied for some range of angles θ_{min} to θ_{max}. Additionally, suppose that all deputies are ejected in some range θ_{min} to θ_{dep} where θ_{dep} is between θ_{min} and θ_{max}. Under these assumptions, duration of the commissioning phase for all deputies must satisfy

$$t_{com} \leq \frac{|\theta_{max} - \theta_{dep}|}{|\dot{\omega}_m|} \tag{39}$$

to ensure that control capability is established before the passive minimum separation in the RN-plane falls below ϵ. Because the precession period of the argument of perigee is on the order of several weeks at minimum, it is clear that commissioning phases of several days are achievable using this procedure. The duration of the commissioning phase can be increased by increasing the separation between spacecraft, which increases the difference between θ_{min} and θ_{max}. Additionally, the commissioning phase can be increased by selecting an orbit near the critical inclination, thereby reducing $\dot{\omega}_m$.

Overall, the proposed deployment procedure provides a means of safely deploying a large number of deputies into an e/i vector separation formation subject to operational constraints and control errors. As compared to the deployment procedure for in-plane swarms, this procedure provides a large increase in the duration of the passively safe relative motion (at least several days), but requires more time and delta-v. Specifically, this procedure can deploy at most one deputy per orbit. Additionally, the delta-v cost of the maneuvers performed by the mothership scales linearly with the number of deputies and the nominal separation as shown in Equation (37). Also, it is noteworthy that the only significant effects of control errors are a reduction in the separation in the relative eccentricity and inclination vector spaces as shown in Equation (38). These effects can be counteracted in the formation design by simply increasing the nominal separation. It follows that the number of spacecraft that can be deployed using this approach is not limited by control errors. Instead, the scalability is limited primarily by operational constraints such as range limits of relative navigation sensors. Additionally, it should be possible to use differential drag control with this formation acquisition procedure because the controller can be allowed several days to negate the relative semimajor axis between the deputies.

VALIDATION SCENARIO DEFINITION

The proposed deployment and formation acquisition procedures for in-plane and e/i vector separation formations are validated using the simulations described in the following. These simulations will demonstrate that the proposed procedures provide passively safe relative motion for sufficient time to allow the deputies to be commissioned in the presence of realistic ejection and maneuver execution errors as well as validate the modeling assumptions used in the previous sections. Each simulation consists of three parts: the open-loop deployment sequence, deputy commissioning, and forced motion control to acquire the final formation. First, the mothership executes the open-loop deployment sequence including ejection of the deputies and

any required maneuvers. Upon ejection from the mothership, each deputy passively drifts for a specified duration to simulate the commissioning phase, allowing operations such as de-spin and sensor and actuator calibration. After the commissioning phase, each deputy engages the described low-thrust control law, which forces the deputy to follow its prescribed guidance profile. The simulations are conducted in an orbit with an altitude of 450 km, an inclination of 20^o, and an eccentricity of 0.002. Each simulation is propagated for one week (approximately 100 orbits) using a high-fidelity numerical orbit propagator including all relevant perturbations in LEO.[24] The perturbation models used by the propagator are included in Table 2.

Table 2. Numerical orbit propagator parameters.

Integrator	Runge-Kutta (Dormand-Prince)
Step size	Fixed: 10 sec
Geopotential	GGM01S (20x20)[25]
Atmospheric density	Harris-Priester[26]
Third body gravity	Lunar and solar point masses, analytical ephemerides
Solar radiation pressure	Satellite cross-section normal to the sun, no eclipses

The swarm is modeled as a micro-satellite mothership and a set of 9 nano-satellite deputies. The mothership is assumed to have a mass of 100 kg, a cross-section area of 1 m^2 and a drag coefficient of 1. The deputy spacecraft are modeled as 3U CubeSats that have a mass of 4.5 kg and a drag coefficient of 0.9. Each deputy is assigned a constant cross-section area of between 0.048 and 0.052 m^2, resulting in differential ballistic coefficients of up to 4% of the ballistic coefficient of the mothership. The sensing and actuation capabilities of the modeled spacecraft are based on commercially available hardware including the Septentrio AsterRx4[27] GNSS receiver, the Busek BET-100[28] electrospray thruster and the P-POD[23] CubeSat deployer. From the performance specifications of these subsystems, the navigation and control performance is modeled as follows. It is assumed that the mothership's 1-σ navigation errors are 5 m and 1 cm/s in position and velocity, respectively, after filtering. Next, it is assumed and that the mothership is able to estimate the mean ROE of each deputy with 1-σ uncertainty of 5 m and a bias of no more than 1 m using the differences in the position, velocity, and time measurements from the GNSS receivers. Additionally, it is assumed that the deployer mechanism has a maximum ejection velocity error of 10% and that the attitude control system of the mothership is able to bound the ejection angle error to within 0.1^o. Finally, a 5% maneuver execution error is applied to both the mothership and the deputies. These navigation and control errors are summarized in Table 3.

Table 3. Simulated navigation and control errors.

Absolute Navigation		Relative Navigation		Control	
Position (1-σ)	5 m	Noise (1-σ)	5 m	Maneuver Execution	5 %
Velocity (1-σ)	1 cm/s	Bias	1 m	Ejection Velocity	10 %
				Ejection Angle	0.1^o

The key parameters for the low-thrust control law are shown in Table 4 and described in the following. The deadband values of 25 m are selected to allow a control error five times larger than the 1-σ relative navigation error. The acceleration produced by the thrusters U is computed from the thrust of the BET-100 and the mass of the modeled spacecraft and U^* is computed according to Equation (18). The reconfiguration time is selected so that the maneuvers performed to correct $\delta\lambda$ after the commissioning phase for the e/i vector separation swarm are on the same order as the cumulative effect of differential drag.

Next, it is necessary to specify the target swarm formations and deployment parameters. Specifically, the formations must be sized to ensure a minimum separation of 125 m between all spacecraft following ejection from the mothership. This separation is selected so that the minimum separation is five times larger than the control deadband. The sizing of the in-plane formation is driven by the need to provide a commissioning

Table 4. Low-thrust control law parameters.

$a\delta\lambda_{db}$	$a\delta e_{db}$	ζ	U	U^*	Δt_{rec}
25 m	25 m	80^o	2.2×10^{-5} m/s^2	1.0×10^{-5} m/s^2	2 days

phase of reasonable duration for all of the deputies. In order to provide a commissioning phase of five orbits for each deputy including the described ejection errors, the selected ejection velocity is 1 m/s (see middle plot in Figure 5). The ejection angle is set at 0.6^o in order to provide sufficient separation from the mothership subject to the worst-case ejection errors. In order to ensure that the mothership has a safe along-track separation from all deputies according to Equation (5), the along-track offset in the guidance profile is set to 3000 m for the in-plane formation. The guidance profile for the relative eccentricity vector for each deputy is obtained by taking the initial value after ejection according to Equation (22) and rotating it at a rate of $\dot{\omega}_m$. The pair of maneuvers used to arrest the drift of the swarm are performed four orbits after the ejection of the first deputy. These maneuvers have a combined delta-v cost of 1.3 cm/s in order to match the nominal along-track component of the ejection velocity in Equation (22). The sizing of the e/i vector separation formation is driven by the need to ensure sufficient separation in the RN-plane over a reasonable range of θ. From Equations (11) and (38), setting $a\delta e_{sep}$ and $a\delta i_{sep}$ to 400 m and the initial value of θ to 30^o is sufficient to ensure a RN-plane separation of 125 m including the errors specified in Table 3. The deputies are ejected with a nominal velocity of 44 cm/s every 1.5 orbits in order to minimize the separation in $\delta\lambda$ produced by the deployment sequence. From Equation (37), the total delta-v cost for the maneuvers performed by the mothership during the deployment sequence is 5.6 m/s. The duration of the commissioning phase for each deputy is four days (61 orbits) in the e/i vector separation formation simulation. In order to assess the modeling assumptions used to derive the constraints on the required separation and the duration of the commissioning phase, the simulations include the worst-case error scenarios for the deployment sequences. Specifically, in the in-plane formation simulation the first deputy is ejected with the maximum possible δa and the last deputy is ejected with the minimum δa. For the e/i vector separation formation simulation, the ejection and maneuver execution errors are specified to produce the minimum possible separation in relative eccentricity vector space between the first and second deputies. The ejection and maneuver execution errors for the remaining deputies are all selected randomly within the range specified in Table 3.

In order to assess the performance of the control law, it is necessary to specify a ground truth reference. The computation sequence used to produce the ground truth mean ROE is shown in Figure 8 and described in the following. First, the absolute position and velocity $\mathbf{x}$ of the mothership and all deputies are numerically integrated using the described orbit propagator including the maneuvers performed by each spacecraft. These trajectories are then converted into osculating orbits. Next, the osculating to mean transformation described by Schaub[29] is applied to the osculating orbits in order to remove short-period oscillations due to J_2. Finally, these mean orbits are used to compute the ground truth mean ROE using Equation (1).

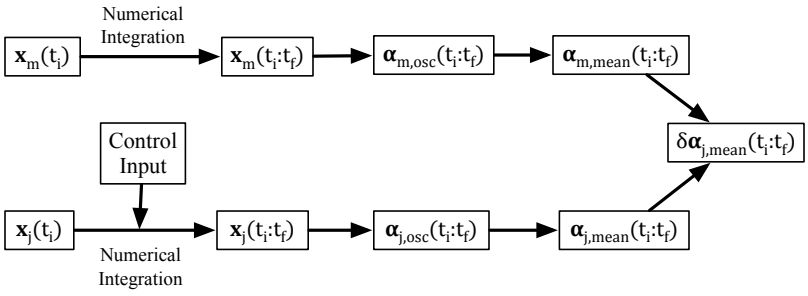

Figure 8. Computation sequence for ground truth mean ROE.

The thrust commands for each deputy are computed from estimates of the absolute state of the mothership

and the mean ROE of each deputy as shown in Figure 9 and described in the following. First, the estimated absolute state of the mothership is computed by adding the described position and velocity noise to the true position and velocity from the numerical propagator. This estimate is converted to an osculating orbit, which is then converted to a mean orbit estimate using Schaub's osculating to mean transformation.[29] The relative state estimate for each deputy is computed by adding the described relative state noise to the ground truth mean ROE. These absolute and relative state estimates are used to compute the commanded thrust for each deputy, which is updated at every ten second time step.

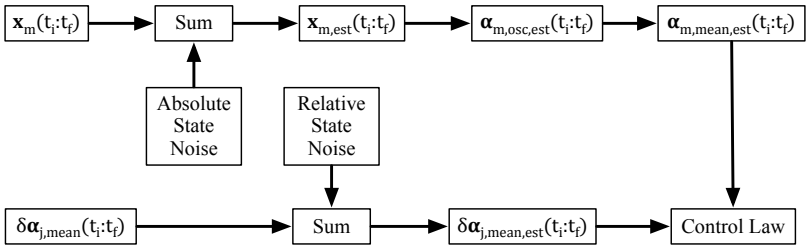

Figure 9. Computation sequence for thrust commands.

RESULTS

The simulation results are assessed using the performance metrics described in the following. The first performance metric is the delta-v cost of the open-loop deployment sequence performed by the mothership, which should be within 5% of the estimated values. The second performance metric is the maximum delta-v cost incurred by any deputy over the complete simulation, which should be on the order of cm/s to counteract the effects of ejection errors and differential drag. The accuracy of the modeling assumptions is assessed using the time history of the minimum separation between any pair of spacecraft. After ejection from the mothership, the minimum separation of each deputy from all other spacecraft should be at least 125 meters. Performance of the control law is assessed using the time histories of $|\delta\lambda_{err}|$ and $||\delta\boldsymbol{e}_{err}||_2$. It is expected that $|\delta\lambda_{err}|$ will converge to the deadband within the specified time of two days. Due to control errors during the deployment sequence, the initial values of $||\delta\boldsymbol{e}_{err}||_2$ will be as large as 100 m for the in-plane swarm simulation and may be larger for the e/i vector separation swarm simulation. However, the distribution of these errors should not compromise the safety of the swarm. It is expected that the periodic maneuvers required to counteract the effects of differential drag, will slowly drive $||\delta\boldsymbol{e}_{err}||_2$ towards the deadband of 25 m over the course of the simulations.

In-Plane Swarm

The delta-v cost incurred during the mothership's open-loop deployment sequence for the in-plane swarm simulation is 1.32 cm/s in agreement with the predicted cost. The largest delta-v cost incurred by any of the deputies is 8.4 cm/s. After ejection from the mothership, all deputies are separated from all other spacecraft by at least 126 m at all times, satisfying the minimum separation requirement. Next, it necessary to assess the accuracy of the model of the minimum separation between the first and last ejected deputies in Equation (36). The minimum separation between the last ejected deputy and all other spacecraft is plotted against the time after ejection in Figure 10. It can be seen that the deputy is within 126 m of another spacecraft exactly one orbit after it is ejected. This corresponds to the closest approach to the mothership as expected since the applied errors result in the smallest acceptable value of δa after ejection. Also, the minimum separation begins to decrease after three orbits to a minimum of 185 meters at the end of the five orbit commissioning phase. This behavior is consistent with the predicted increase in the relative mean longitude between the first and last deployed deputies over the commissioning phase. After the control law is engaged, the minimum separation between any pair of spacecraft is held at a stable 600 m, which is equal to the nominal separation in relative eccentricity vector space.

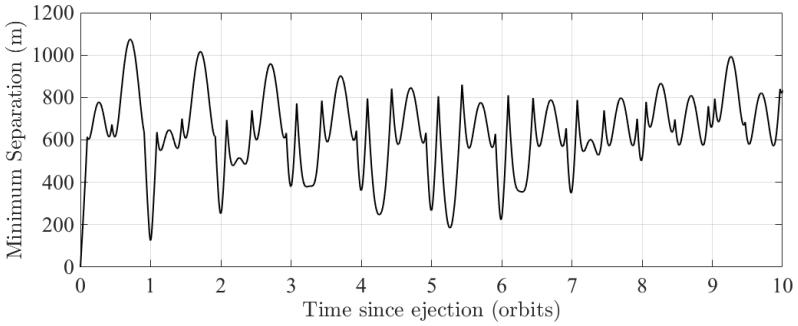

Figure 10. Time history of minimum separation of last ejected deputy from all other spacecraft for in-plane formation simulation.

Next, consider the time history of $|\delta\lambda_{err}|$ and $||\delta \boldsymbol{e}_{err}||_2$ for each deputy over the forced motion control phase as shown in Figure 11. It can be seen that $|\delta\lambda_{err}|$ converges to within the deadband in less than 7 orbits, which corresponds to 0.5 days. This is much faster than the specified two day reconfiguration time and is similar to the behavior seen in the authors' previous work.[7] This is because the introduction of navigation errors causes the control law to perform larger maneuvers than expected. Specifically, when the spacecraft is in the deadband of the control law, but close to the switching line, the navigation errors will sometimes cause a commanded maneuver. Also, there are two deputies that have initial relative eccentricity vector errors of 100 meters. These are the first and last ejected deputies, which are subject to the largest possible ejection errors. All deputies are able to reduce the eccentricity vector error to within the 25 meter deadband by the end of the one week simulation.

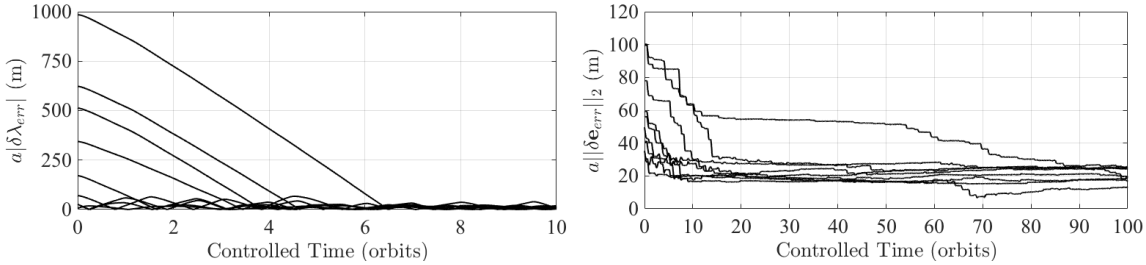

Figure 11. Time history of $|\delta\lambda_{err}|$ (left) and $||\delta e_{err}||_2$ (right) for each deputy during forced motion control phase for in-plane formation simulation.

E/I Vector Separation Swarm

The delta-v cost incurred during the mothership's open-loop deployment sequence for the e/i vector separation swarm simulation is 5.8 m/s, which is only slightly larger than the predicted value of 5.6 m/s. The largest delta-v cost incurred by any of the deputies is 12 cm/s. Next, it is necessary to validate the assumption that the ejection angle error has negligible impact on the deployment sequence. The minimum separation between the first ejected deputy and all other spacecraft is plotted against the time since ejection in Figure 10. The minimum separation between this deputy and all other spacecraft in only the RN-plane is included as a dotted line. It can be seen that the minimum separation reaches a local minimum 0.5 orbits after ejection. A reduced separation is expected at this stage as the mothership has only performed one maneuver to establish separation from the deputy in relative eccentricity vector space. After one complete orbit, the minimum separation between this deputy and any other spacecraft is always 182 m or larger. However, when only separation in the RN-plane is considered, there are stable local minima in the minimum separation of

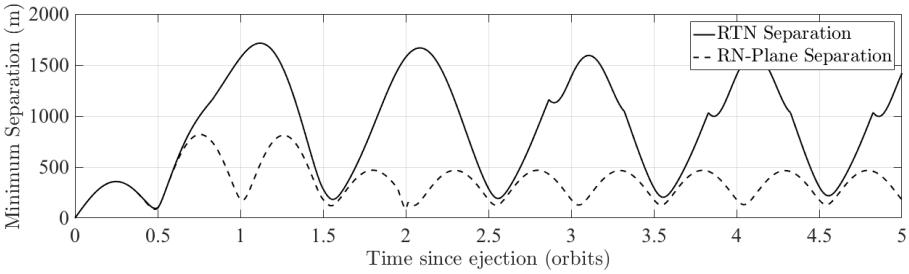

Figure 12. Time history of minimum separation of first ejected deputy from all other spacecraft for e/i vector separation formation simulation.

approximately 120 m starting 1.5 orbits after ejection. This is only slightly smaller than the predicted value of 125 m, validating the assumption that the effects of ejection angle errors can be neglected. Overall, these results are consistent with the analytical models and demonstrate that this deployment procedure can provide several days of passively safe relative motion including ejection and maneuver execution errors.

The evolutions of $|\delta\lambda_{err}|$ and $||\delta \boldsymbol{e}_{err}||_2$ for each deputy in this simulation are shown in Figure 13. The trends in these plots are very similar to those in Figure 11. After the control law is engaged, $|\delta\lambda_{err}|$ is reduced to the 25 m deadband for all deputies in 20 orbits (approximately 1.3 days) or less, which is still faster than the specified reconfiguration time of 2 days. The larger initial values of $|\delta\lambda_{err}|$ are due to the effects of differential drag over the four day commissioning phase. Also, the initial values of $||\delta \boldsymbol{e}_{err}||_2$ are as large as 130 m. However, most of these errors are reduced to 25 m by the end of the simulation and the remainder are strictly decreasing once the control law is engaged.

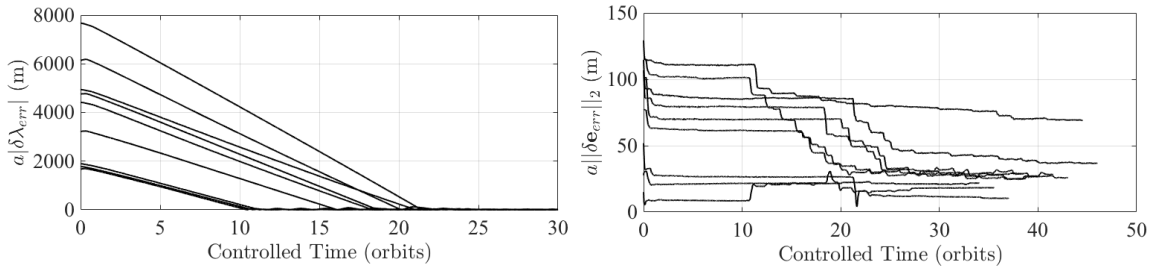

Figure 13. Time history of $|\delta\lambda_{err}|$ (left) and $||\delta \boldsymbol{e}_{err}||_2$ (right) for each deputy during forced motion control phase for e/i vector separation formation simulation.

Overall, these results demonstrate that the proposed deployment formation acquisition procedures are able to safely initialize both in-plane and e/i vector separation formations including realistic control errors and operational constraints. Additionally, the evolution of the minimum separation between spacecraft shows very strong agreement with the trends predicted by the analytical models. Thus, these models can be used by mission designers to quickly asses how different design variables affect the behavior of these swarms during initial mission phases.

CONCLUSION

In addition to the formation-keeping and reconfiguration techniques in literature, spacecraft swarm missions will require safe and robust initialization procedures. To meet this need, this paper presents two deployment and formation acquisition procedures that enable a mothership to deploy a large number of deputies into passively safe formations subject to operational constraints and control errors. Additionally, analytical lower bounds on the duration of the passively safe relative motion after ejection from the mothership are derived for

each of these procedures as functions of the control error parameters. These bounds are used to specify the allowable duration of commissioning operations for the deputies. For the in-plane formation deployment procedure, the duration of the passively safe relative motion is generally less than one day and depends strongly on both the ejection angle error and the number of deputies. As a result, sub-degree attitude control precision for the mothership will be required to minimize the difference in orbit energy between ejected deputies. Instead, the deployment procedure for e/i vector separation formations is is able to guarantee several days or more of passively safe relative motion regardless of the number of deputies, suggesting that use of differential drag control is feasible. Additionally, this deployment procedure can be used to minimize risk at no cost to mission performance because the formation can be arbitrarily reconfigured once actuation capabilities are established on the deputies. The cost of the increase in passive safety is that the deployment procedure is slower and incurs a larger delta-v cost for the mothership.

The performance of the proposed formation acquisition procedures is validated through simulations using a high-fidelity numerical orbit propagator. It is found that the observed trends in the minimum separation distance between spacecraft over the simulation agree with the predicted trends from the analytical models. Specifically, the minimum separation for the in-plane formation simulation shows a steady decrease every orbit until the end of the commissioning phase as expected due to the relative drift between deployed deputies. Additionally, the delta-v costs for any spacecraft are no more than 8.4 cm/s over the entire one week simulation. For the e/i vector separation swarm simulation, the minimum separation in the plane perpendicular to the flight direction is within 5 m of the predicted value of 125 m. The delta-v cost of acquiring this formation is 5.8 m/s for the mothership, but this cost allows the deputies to take several days to perform commissioning operations with no risk of collision. All of these delta-v costs are small relative to the capacity of current propulsion systems, suggesting that these deployment procedures can be used in a wide range of mission applications.

The presented deployment and formation acquisition procedures are subject to two key limitations. First, the models used to compute the minimum separation between spacecraft are only valid for near-circular orbits. Second, contingencies for maneuver or ejection failures are not addressed. Future works will apply the same approach to eccentric orbits and assess the risks posed by maneuver and ejection failures, ensuring that swarm formations can be safely established in any orbit.

ACKNOWLEDGMENT

This work was supported by a NASA Office of the Chief Technologists Space Technology Research Fellowship (NSTRF), NASA Grant #NNX15AP70H and the King Abdulaziz City for Science and Technology (KACST).

REFERENCES

[1] B. D. Tapley, S. Bettadpur, M. Watkins, and C. Reigber, "The gravity recovery and climate experiment: Mission overview and early results," *Geophysical Research Letters*, Vol. 31, No. 9, 2004.

[2] G. Krieger, A. Moreira, H. Fiedler, I. Hajnsek, M. Werner, M. Younis, and M. Zink, "TanDEM-X: A Satellite Formation for High-Resolution SAR Interferometry," *IEEE Transactions on Geoscience and Remote Sensing*, Vol. 45, No. 11, 2007, pp. 3317–3341.

[3] J. L. Burch, T. E. Moore, R. B. Torbert, and B. L. Giles, "Magnetospheric Multiscale Overview and Science Objectives," *Space Science Reviews*, Vol. 199, No. 1, 2016, pp. 5–21.

[4] S.-J. Chung and F. Y. Hadaegh, "Swarms of Femtosats for Synthetic Aperture Applications," *Proceedings of the Fourth International Conference on Spacecraft Formation Flying Missions & Technologies, St. Hubert, Quebec, May 18-20*, 2011.

[5] M. E. Campbell, "Collision Monitoring within Satellite Clusters," *IEEE Transactions on Control Systems Technology*, Vol. 13, No. 1, 2005, pp. 42–55.

[6] D. Morgan, S.-J. Chung, L. Blackmore, B. Acikmese, D. Bayard, and F. Y. Hadaegh, "Swarm-Keeping Strategies for Spacecraft Under J_2 and Atmospheric Drag Perturbations," *Journal of Guidance, Control, and Dynamics*, Vol. 35, No. 5, 2012, pp. 1492–1506.

[7] A. W. Koenig and S. D'Amico, "Robust and Safe N-Spacecraft Swarming in Perturbed Near-Circular Orbits," *26th International Symposium on Space Flight Dynamics, June 3-9, Matsuyama, Japan*, 2017.

[8] M. E. Campbell, "Planning Algorithm for Multiple Satellite Clusters," *Journal of Guidance, Control, and Dynamics*, Vol. 26, No. 5, 2003, pp. 770–780.

[9] D. Morgan, *Guidance and Control of Swarms of Spacecraft*. PhD thesis, University of Illinois at Urbana-Champaign, 2015.

[10] S. Bandyopadhyay, S.-J. Chung, and F. Y. Hadaegh, "Probabilistic and Distributed Control of a Large-Scale Swarm of Autonomous Agents," *IEEE Transactions on Robotics*, 2016. Submitted.

[11] D. Morgan, G. P. Subramanian, S.-J. Chung, and F. Y. Hadaegh, "Swarm Assignment and Trajectory Optimization using Variable-Swarm, Distributed Auction Assignment and Sequential Convex Programming," *The International Journal of Robotics Research*, Vol. 35, No. 10, 2016, pp. 1261–1285.

[12] M. Kirschner, O. Montenbruck, and S. Bettadpur, "Flight dynamics aspects of the GRACE formation flying," *2nd International Workshop on Satellite Constellations and Formation Flying*, 2001, pp. 19–20.

[13] E. Gill, O. Montenbruck, and S. D'Amico, "Autonomous formation flying for the PRISMA mission," *Journal of Spacecraft and Rockets*, Vol. 44, No. 3, 2007, pp. 671–681.

[14] M. Wermuth, G. Gaias, and S. D'Amico, "Safe Picosatellite Release from a Small Satellite Carrier," *Journal of Spacecraft and Rockets*, Vol. 52, No. 5, 2015, pp. 1338–1347.

[15] A. Boutonnet, V. Martinot, A. Baranov, and B. Escudier, "Optimal Invariant Spacecraft Formation Deployment with Collision Risk Management," *Journal of Spacecraft and Rockets*, Vol. 42, No. 5, 2005, pp. 913–920.

[16] S. D'Amico and O. Montenbruck, "Proximity Operations of Formation-Flying Spacecraft Using an Eccentricity/Inclination Vector Separation," *Journal of Guidance, Control, and Dynamics*, Vol. 29, No. 3, 2006, pp. 554–563.

[17] S. D'Amico, *Autonomous Formation Flying in Low Earth Orbit*. PhD thesis, Delft University of Technology, 2010.

[18] A. W. Koenig, T. Guffanti, and S. D'Amico, "New State Transition Matrices for Spacecraft Relative Motion in Perturbed Orbits," *Journal of Guidance, Control, and Dynamics*, 2017. DOI: 10.2514/1.G002409.

[19] S. D'Amico, "Relative Orbital Elements as Integration Constants of Hills Equations," *DLR, TN 05-08*, 2005.

[20] F. deBruijn, E. Gill, and J. How, "Comparative Analysis of Cartesian and Curvilinear Clohessy-Wiltshire equations," *Journal of Aerospace Engineering, Sciences and Applications*, Vol. 3, No. 2, 2011, pp. 1–15.

[21] G. Gaias and S. D'Amico, "Impulsive Maneuvers for Formation Reconfiguration Using Relative Orbital Elements," *Journal of Guidance, Control, and Dynamics*, Vol. 38, No. 6, 2014, pp. 1036–1049.

[22] M. Chernick and S. D'Amico, "New Closed-Form Solutions for Optimal Impulsive Control of Spacecraft Relative Motion," *AIAA/AAS Astrodynamics Specialist Conference, Long Beach, California, September 13-16*, 2016.

[23] J. Puig-Suari, C. Turner, and W. Ahlgren, "Development of the Standard CubeSat Deployer and a CubeSat Class PicoSatellite," *Proceedings of the 2001 Aerospace Conference*, Vol. 1, IEEE, 2001, pp. 347–353.

[24] D. Eddy, V. Giralo, and S. D'Amico, "Development and Verification of the Stanford GNSS Navigation Testbed for Spacecraft Formation-Flying," Technical Note, 2017. URL: https://people.stanford.edu/damicos/sites/default/files/tn2017_eddygiralodamico.pdf.

[25] B. D. Tapley, F. Flechtner, S. V. Bettadpur, and M. M. Watkins, "The status and future prospect for GRACE after the first decade," *AGU Fall Meeting Abstracts*, Vol. 1, 2013, p. 01.

[26] O. Montenbruck and E. Gill, *Satellite orbits: Models, Methods and Applications*. Springer Science & Business Media, 2012.

[27] E. van Rees, "Septentrio Satellite Navigation," *GeoInformatics*, Vol. 18, No. 4, 2015, p. 10.

[28] Busek Co. Inc., "Busek BET-100 Datasheet," URL: http://www.busek.com/index_htm_files/70008516F.pdf.

[29] H. Schaub and J. L. Junkins, *Analytical Mechanics of Space Systems*. AIAA, 2003.